Radiation Measurements 135 (2020) 106334

Contents lists available at ScienceDirect

Radiation Measurements

journal homepage: http://www.elsevier.com/locate/radmeas

TL/OSL signal of $CaSO_4$:Eu,Ag samples produced by variations of the slow evaporation route

Danilo O. Junot [a,*], Divanizia N. Souza [b], Linda V.E. Caldas [a]

[a] Instituto de Pesquisas Energéticas e Nucleares/Comissão Nacional de Energia Nuclear, São Paulo, SP, Brazil
[b] Departamento de Física, Universidade Federal de Sergipe, São Cristóvão, SE, Brazil

ARTICLE INFO

Keywords:
$CaSO_4$ synthesis methods
Radiation dosimetry
Thermoluminescence
Optically stimulated luminescence

ABSTRACT

The aim of this work was to produce crystals of $CaSO_4$ doped with europium (Eu) and silver (Ag) nanoparticles, by means of three different preparation routes, and to study their applicability in radiation dosimetry by the TL and OSL techniques. The crystals were produced by variations of the slow evaporation route. Samples of $CaSO_4$:Eu,Ag(a) were obtained using europium oxide and silver particles as dopants. For the growth of the crystals of $CaSO_4$:Eu,Ag(b), silver was incorporated in nitrate form. $CaSO_4$:Eu,Ag(c) phosphorus were synthetized mixing europium oxide in a colloidal suspension of silver nanoparticles. Optical characterization confirmed the presence of Eu^{3+}/Eu^{2+} in the crystal matrix. Dosimetric characteristics were evaluated after the exposure of the samples to a $^{90}Sr/^{90}Y$ source. The $CaSO_4$:Eu,Ag(a) and $CaSO_4$:Eu,Ag(b) composites presented the most intense signals, the lowest detectable doses, and showed a linear and reproducible dose response, but the $CaSO_4$:Eu,Ag(a) samples showed the best potential for application in TL/OSL dosimetry.

1. Introduction

The techniques of thermoluminescence (TL) and optically stimulated luminescence (OSL) are highly sensitive to defects caused by external elements to the crystalline matrix of a luminescent material. The structure of these defects can be controlled by the matrix preparation method (Azorin, 2014). The application of $CaSO_4$:RE (RE = rare earth) phosphors in TL dosimetry of radiation originated in the 1970s, when Yamashita et al. (1971) proposed an efficient and relatively simple method for doping $CaSO_4$ using rare earths.

Lakshmanan (1999) performed a systematic study of $CaSO_4$ doped with all lanthanides and observed that the highest sensitivities were presented by $CaSO_4$:Tm and $CaSO_4$:Dy. However, Ingle et al. (2008) and Kher et al. (2011) observed that europium (Eu) is also a promising activator, and several studies have been carried out with europium doped calcium sulphate ($CaSO_4$:Eu).

Although the TL sensitivity of many materials is found to decrease when they are synthesized in a nanometric scale, silver (Ag) nanoparticles were used to improve the luminescent characteristics in some semiconductor materials. Junot et al. (2011) observed that the incorporation of silver into $CaSO_4$:Eu enables more intense (about 4x higher) TL and thermally stimulated exoelectronic emissions (TSEE) than in the silverless material, especially when silver was incorporated as a co-dopant in the form of nanoparticle agglomerates. The TL emission curves reported by Junot et al. (2011, 2014) for $CaSO_4$:Eu and $CaSO_4$:Eu,Ag are identical, with only differences in their signal intensity.

Kulkarni et al. (2014) and Guckan et al. (2017) made a systematic study of the OSL response of $CaSO_4$ phosphates doped with europium, but there are no reports on the use of $CaSO_4$:Eu,Ag in this type of dosimetry. Yashaswini et al. (2017) also evaluated the photoluminescence of $CaSO_4$ nanoparticles, but these authors did not explain the physical phenomena caused by the reduced size of the particle. Thus, the mechanisms of formation of defects related to the insertion of silver in the matrix are still unknown, and any advance to explain the behaviour of these defects in these materials is relevant, as there are still few studies about the mechanisms of charge compensation and luminescent centres in $CaSO_4$ matrices (Kudryavtseva et al., 2014). Besides that, it is extremely important to advance on research that allows the development of sensitive and low-cost TL/OSL dosimeters, competing with those available in the market.

Therefore, the aim of this work was to produce crystals of $CaSO_4$ doped with europium (Eu) and silver (Ag) nanoparticles, by means of three different variations of the slow evaporation route, and to compare their dosimetric properties in order to achieve the best production

* Corresponding author.
E-mail address: dan.junot@gmail.com (D.O. Junot).

https://doi.org/10.1016/j.radmeas.2020.106334
Received 30 October 2019; Received in revised form 21 March 2020; Accepted 1 April 2020
Available online 15 April 2020

procedure for applicability in radiation dosimetry by the TL and OSL techniques.

2. Experimental procedure

The production of the composites used in this work was carried out through three stages:

1. Synthesis of the silver particles used as dopants: the silver particle agglomerates were obtained by the polyol method, which is based on the silver reduction from the precursor agent ($AgNO_3$) by the reducing agent ($NaBH_4$). Details of the silver particles synthesis can be found in Junot et al. (2014);
2. Growth of the $CaSO_4$ crystals: the crystals were produced by variations of the slow evaporation route. All preparations were based on the mixture of calcium carbonate ($CaCO_3$), sulfuric acid (H_2SO_4) and dopant oxide (Eu_2O_3) in 0.1 mol% of $CaCO_3$ mass concentration. To obtain the crystals, the solution of $CaSO_4$+H_2SO_4+H_2O + dopants, resulting from the mixture, was deposited in a beaker and remained in the magnetic stirrer at 120 °C until complete homogenization and evaporation of the water. Subsequently the solution was introduced into a volumetric flask on a heating blanket at 375 °C until all the acid evaporated. Acid vapours were condensed and were collected in an Erlenmeyer flask at the outlet of the condenser, providing reuse of the acid. Possible non-condensed vapours were conducted to wash bottles containing 250 ml of sodium hydroxide solution to be neutralized. The crystals were grown in a sealed vacuum system. Samples of $CaSO_4$:Eu,Ag(a) were obtained using silver particles, produced by the polyol method, as dopants. For the growth of the crystals of $CaSO_4$:Eu,Ag(b), silver was incorporated in nitrate form, dissolved in water. $CaSO_4$:Eu,Ag(c) phosphorus were synthetized mixing europium oxide in a colloidal suspension of silver nanoparticles dispersed in ethylene glycol;
3. Production of the pellets: they were made from 75 to 150 μm crystal grains by adding 50% mass of polytetrafluoroethylene (Teflon) to improve the strength of the material. The pellets produced were subjected to a uniaxial pressure of 2 tons and sintered at 400 °C for 1 h. After sintering, the pellets presented 1 mm in thickness, 6 mm in diameter and 40 mg mass.

The samples were exposed to a beta radiation source ($^{90}Sr/^{90}Y$ from Risö TL/OSL reader, at a rate of 81 mGy/s) at a dose range from 0.081 Gy to 50 Gy.

X-ray diffraction measurements were performed in a Rigaku diffractometer of Bragg-Brentano geometry using Cu-Kα radiation. The continuous mode was used with a scan range of 20–80°, scan step of 0.02 and scan speed of 2°/min.

TL analyses were performed in a Risö TL/OSL reader using different heating rates in the range from 1 °C/s to 10 °C/s, to a maximum temperature of 400 °C. OSL measurements were also carried out in the Risö TL/OSL reader. For the excitation of the samples, blue LEDs (Light Emitting Diodes), with emission at 470 nm, and continuous-wave mode were used. In order to carry out measurements of the TL emission spectra, a high resolution spectrometer from Ocean Optics was coupled in place of the photomultiplier.

The TL response reproducibility of the samples was determined using 50 pellets from each material. The pellets were irradiated with 1 Gy ($^{90}Sr/^{90}Y$), evaluated at the TL reader at a heating rate of 10 °C/s, thermally treated and irradiated again. This cycle was carried out 5 times and, after each cycle, the pellets were treated thermally during 1 h at 400 °C.

All results in this work represent the average of at least three different measurements, in order to minimize the uncertainties.

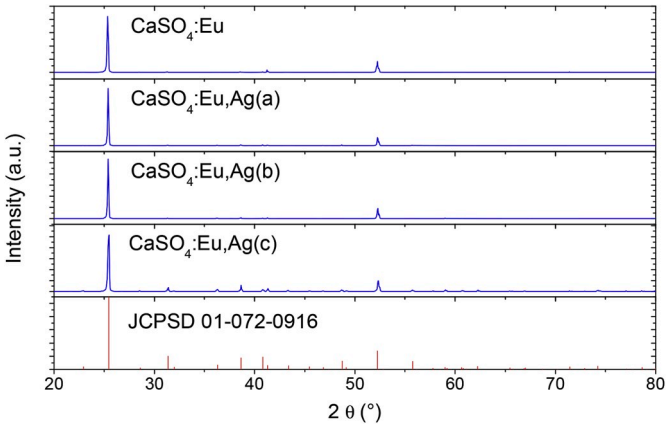

Fig. 1. X-ray diffraction of crystalline samples of $CaSO_4$:Eu, $CaSO_4$:Eu,Ag(a), $CaSO_4$:Eu,Ag(b) and $CaSO_4$:Eu,Ag(c), in comparison to the pattern.

3. Results and discussion

3.1. X-ray diffraction analysis (XRD)

Fig. 1 shows the XRD results for the prepared samples, in powder form, after calcination. The diffraction patterns obtained for all samples showed diffraction peaks and relative intensities corresponding to the anhydride structure (JCPSD 01-072-0916). Thus, it can be observed that the samples of doped $CaSO_4$ presented only a single phase, which was expected, since the technique does not allow to observe the presence of dopants in concentrations less than 5%.

3.2. TL emission spectra

The emission spectrum of the $CaSO_4$:Eu samples irradiated with absorbed dose of 50 Gy is shown in Fig. 2. Emissions can be observed corresponding to the Eu^{2+} ions (with emission at 380 nm) and those corresponding to Eu^{3+}, that emits at 590 nm ($^5D_0 \rightarrow {}^7F_1$), 614 nm ($^5D_0 \rightarrow {}^7F_2$) and 695 nm ($^5D_0 \rightarrow {}^7F_4$), denoting that both ions were incorporated into the $CaSO_4$ matrix. During heating, these samples presented a red coloration, corresponding to the 614 nm main emission. It can be noticed that the recombination centres related to Eu^{2+} ions are associated to shallow traps, and the recombination centres related to Eu^{3+} ions are associated to deeper traps, since their TL main emissions occur at 175 °C and 300 °C, respectively.

The emission spectra of the $CaSO_4$:Eu,Ag(a), $CaSO_4$:Eu,Ag(b) and $CaSO_4$:Eu,Ag(c) samples are shown in Fig. 3,Figs. 4 and 5, respectively. It is possible to observe the emissions corresponding to the Eu^{2+} ions, and, very weakly, the emissions corresponding to the Eu^{3+} ions. The $CaSO_4$:Eu,Ag(c) samples also showed unexpected emissions at 450 nm and 500 nm (an emission band between 475 nm and 525 nm). It is presumed that because these samples were produced with the addition of new elements (such as ethylene glycol), other impurities have been incorporated into the $CaSO_4$ matrix, possibly carbon. During the heating, all silver doped samples showed a low violet colour, since its main emission occurs in the ultraviolet/violet edge (380 nm). Comparing the spectra, it is possible to observe that the presence of silver drastically reduces the concentration of recombination centres associated with the trivalent europium (with main emission at 614 nm) and increases the concentration of recombination centres associated with the divalent ion (with emission at 380 nm). This can be confirmed by observing the spectra only over the ultraviolet region.

3.3. Glow curves

Fig. 6 shows the TL glow curves of the $CaSO_4$:Eu, $CaSO_4$:Eu,Ag(a), $CaSO_4$:Eu,Ag(b) and $CaSO_4$:Eu,Ag(c) composites after irradiation with 1

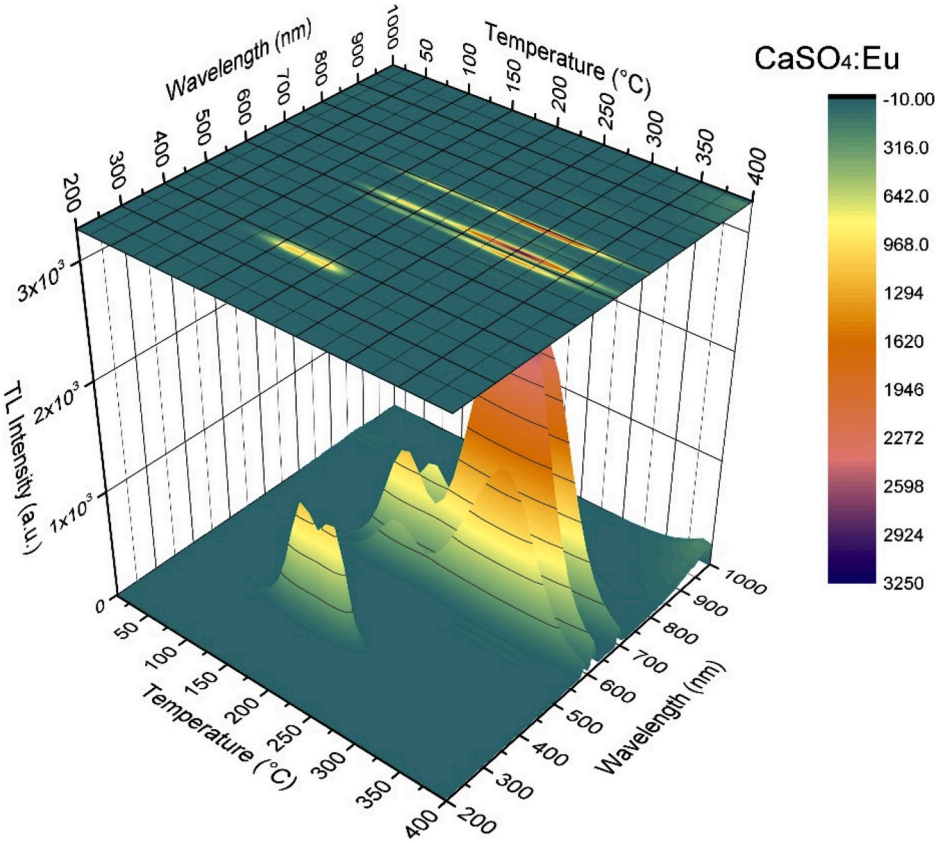

Fig. 2. TL emission spectrum of the $CaSO_4$:Eu samples, after irradiation with 50 Gy ($^{90}Sr/^{90}Y$).

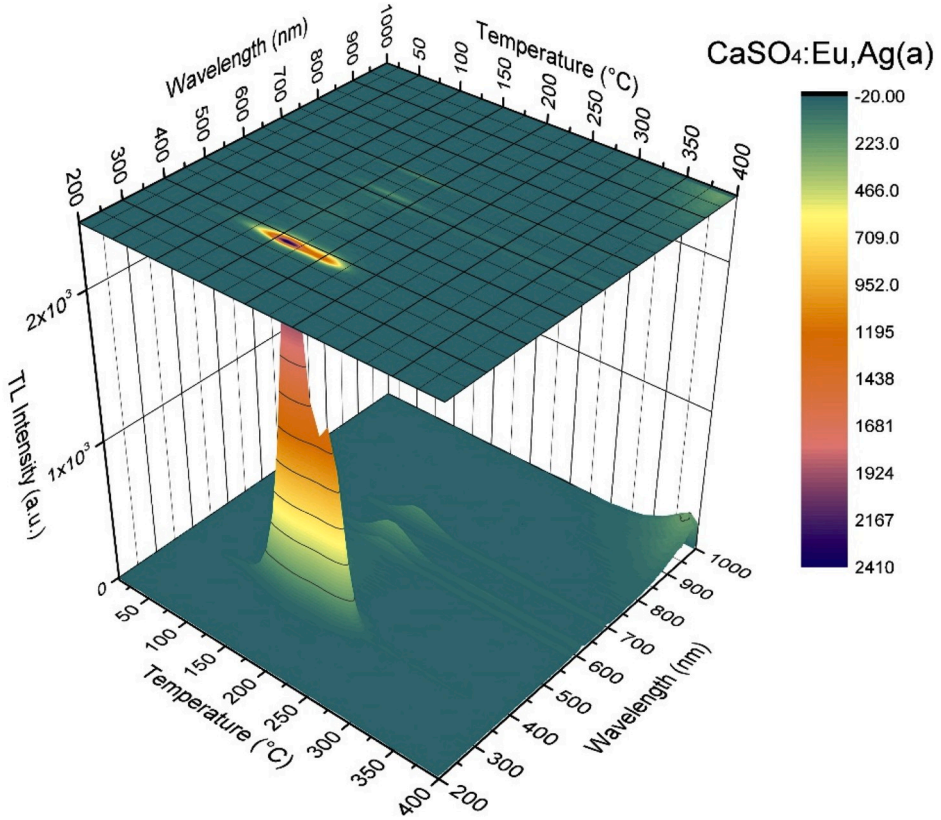

Fig. 3. TL emission spectrum of the $CaSO_4$:Eu,Ag(a) samples, after irradiation with 50 Gy ($^{90}Sr/^{90}Y$).

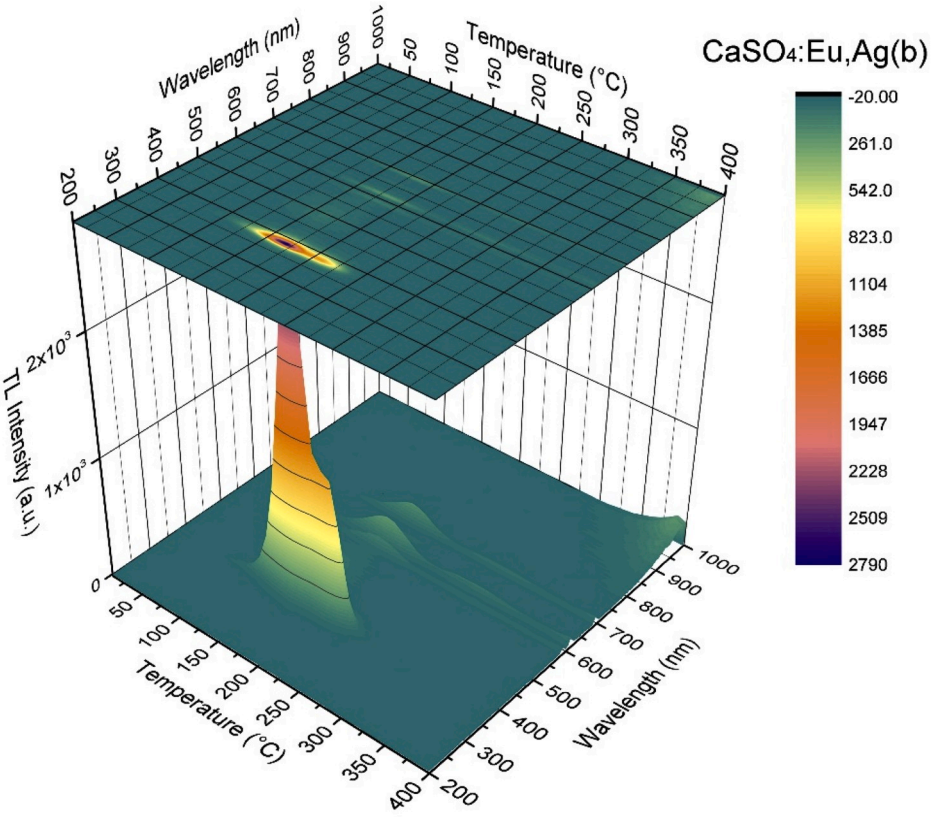

Fig. 4. TL emission spectrum of the $CaSO_4$:Eu,Ag(b) samples, after irradiation with 50 Gy ($^{90}Sr/^{90}Y$).

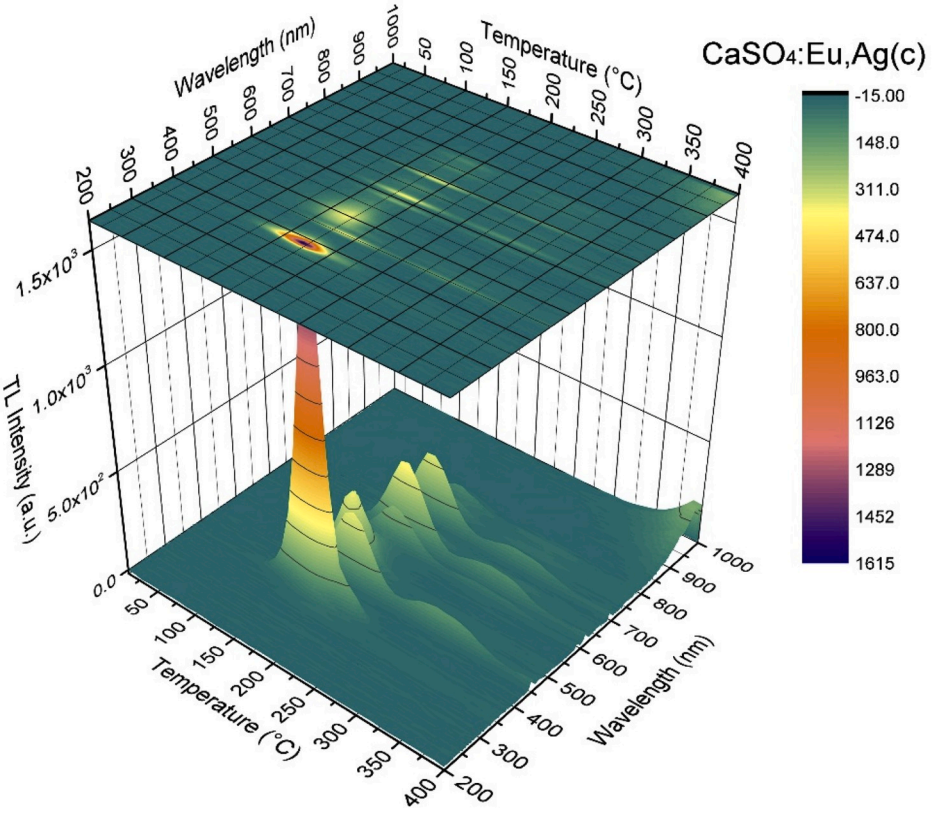

Fig. 5. TL emission spectrum of the $CaSO_4$:Eu,Ag(c) samples, after irradiation with 50 Gy ($^{90}Sr/^{90}Y$).

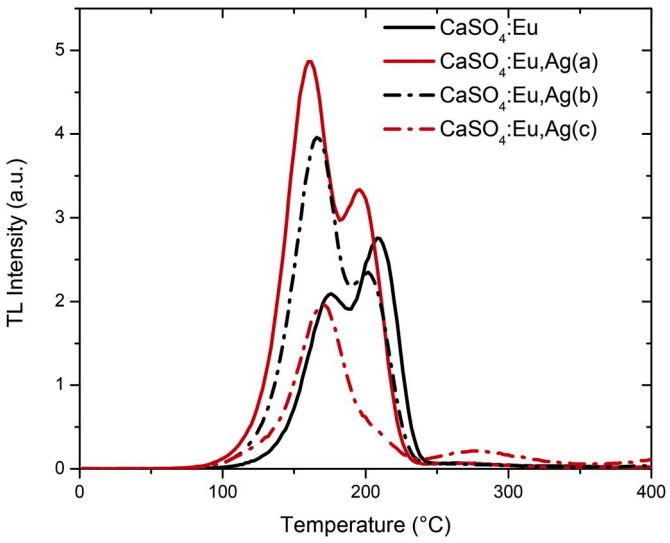

Fig. 6. Typical TL glow curves of $CaSO_4$:Eu, $CaSO_4$:Eu,Ag(a), $CaSO_4$:Eu,Ag(b) and $CaSO_4$:Eu,Ag(c) samples due to an absorbed dose of 1Gy from a $^{90}Sr/^{90}Y$ source.

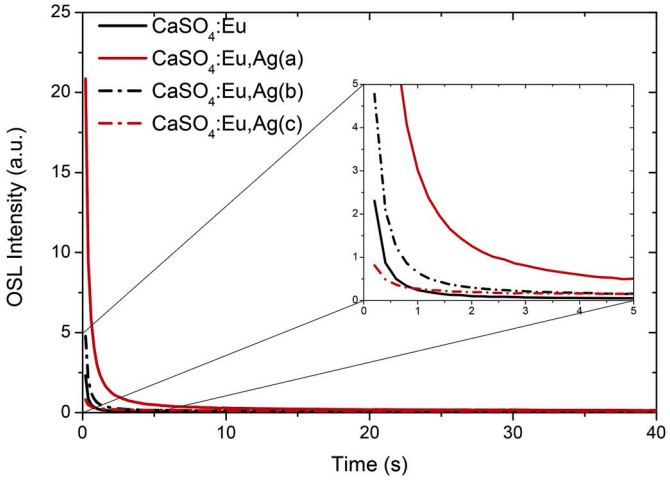

Fig. 7. OSL emission curves of $CaSO_4$:Eu, $CaSO_4$:Eu,Ag(a), $CaSO_4$:Eu,Ag(b) and $CaSO_4$:Eu,Ag(c) samples irradiated with 1 Gy ($^{90}Sr/^{90}Y$).

Gy. The heating rate used in the readings was 10 °C/s. It can be observed that all the composites present TL responses between 130 °C and 230 °C, with the maximum intensity at around 170 °C for silver co-doped samples and 205 °C for the $CaSO_4$:Eu samples. Surprisingly, the $CaSO_4$:Eu,Ag(c) samples also showed a low intensity peak at 280 °C. The $CaSO_4$:Eu,Ag(a) samples showed a considerably more intense emission, about 2 times higher than the $CaSO_4$:Eu samples. Junot et al. (2011, 2014) have already reported more intense TL emission curves in silver co-doped samples. As observed in the TL emission spectra, the explanation for the higher sensitivity of $CaSO_4$:Eu,Ag is that the photomultiplier (PMT) used in TL reading has a higher quantum efficiency (or sensitivity) for wavelengths in the ultraviolet-blue region than for wavelengths in the region of the red colour (Risö, 2015) and, as the spectra show (Figs. 3–5), the emission of co-doped silver samples occurs almost entirely in the ultraviolet/violet region. It is also due to this fact that the high intense peak at 300 °C that appears in the $CaSO_4$:Eu TL emission spectrum cannot be seen in the $CaSO_4$:Eu TL glow curve, since the PMT sensitivity is just from 200 nm to 600 nm. It is important to notice that no emission related to Ag ions can be observed. So, it is clear that the insertion of silver enhances the concentration of Eu^{2+} ions in the

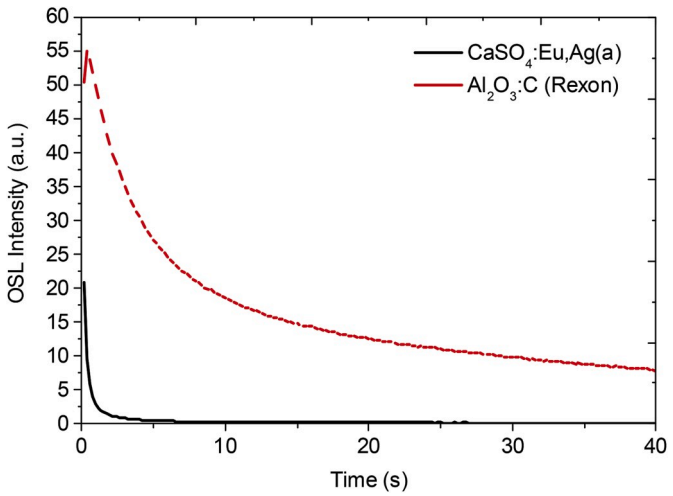

Fig. 8. Comparison between the OSL emissions of the $CaSO_4$:Eu,Ag(a) and the Al_2O_3:C (Rexon) samples irradiated with 1 Gy ($^{90}Sr/^{90}Y$).

$CaSO_4$ lattice and, consequently, the TL emission collected by the Risö TL/OSL reader. The $CaSO_4$:Eu,Ag(c) samples showed a different glow curve behaviour from the other samples containing silver, which strengthens the hypothesis that there are impurities in these samples.

Fig. 7 shows the OSL curves with an integration time of 40 s for the $CaSO_4$:Eu, $CaSO_4$:Eu,Ag(a), $CaSO_4$:Eu,Ag(b) and $CaSO_4$:Eu,Ag(c) samples, after an absorbed dose of 1 Gy. The composites present intense signals, due to their high sensitivity. The samples show exponential decay as the optically active traps are emptied, which indicates that the traps responsible for the OSL emission have high photoionization cross sections for the 470 nm wavelength of the blue LEDs. The $CaSO_4$:Eu,Ag (a) sample presented the highest OSL intensity, about 4 times higher than the OSL intensity of $CaSO_4$:Eu,Ag(b). As expected, both samples show high potential for use in OSL dosimetry. Fig. 8 shows a comparison between the OSL emissions of the $CaSO_4$:Eu,Ag(a) samples and the commercial Al_2O_3:C samples produced by Rexon. They were irradiated with 1 Gy ($^{90}Sr/^{90}Y$) prior to measurement. The OSL curves of the two composites are very different. The $CaSO_4$:Eu,Ag(a) OSL signal presented a fast decay component predominance, while the Al_2O_3:C (Rexon) OSL signal presented a greater significance of medium to slow decay components. By considering the initial OSL signal (first channel), the $CaSO_4$:Eu,Ag(a) samples presented around 40% of the Al_2O_3:C intensity. On the other hand, by considering the total area under the OSL curve, the $CaSO_4$:Eu,Ag(a) samples presented only around 5% of the commercial Al_2O_3:C response.

With the aim of investigating the optical stimulation influence on the TL emission curve of the dosimeters and to verify the relationship between the TL peaks and the OSL emission, consecutive TL → OSL and OSL → TL measurements were performed only in the $CaSO_4$:Eu,Ag(a) samples, due to its considerably higher TL/OSL intensities. The TL/OSL responses obtained for the $CaSO_4$:Eu,Ag(a) samples are shown in Fig. 9. The previous TL reading reduces almost completely the OSL signal of the samples and the previous OSL reading significantly reduces the subsequent TL signal, especially of the lowest temperature peak. This makes it clear that the luminescent centres of the Eu^{2+} ions present in the sample have a high photoionization cross section for the blue LED employed (470 nm), and that these centres are responsible for both the TL and the OSL signals.

3.4. Reproducibility and linearity

To study the reproducibility of the composites, the pellets were irradiated with 1 Gy, evaluated at the TL reader, thermally treated and irradiated again. This cycle was carried out 5 times. However, due to the

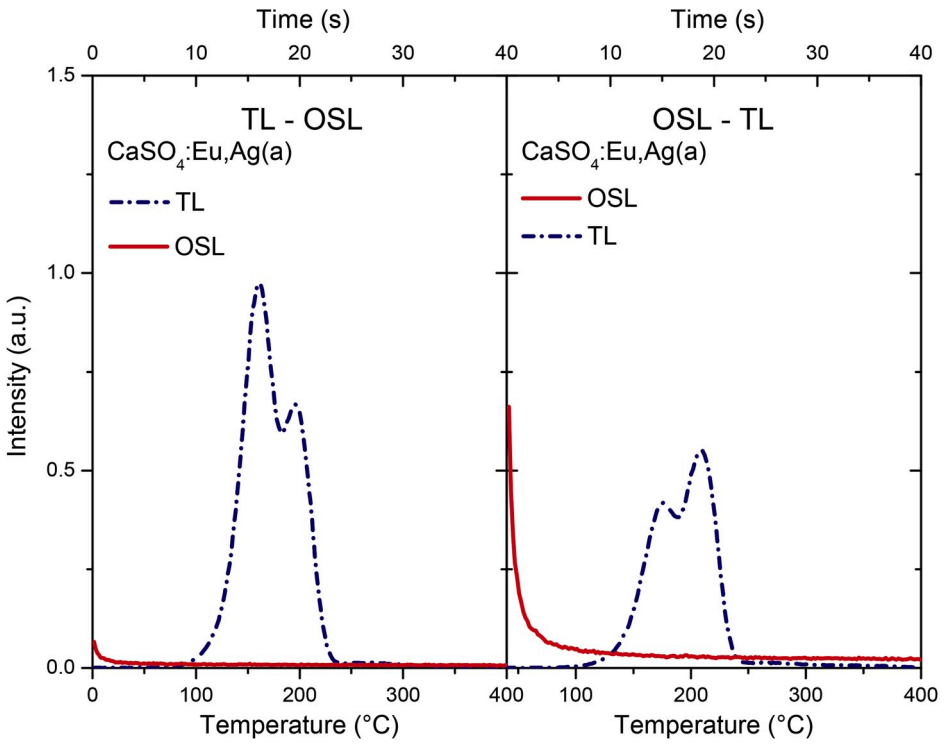

Fig. 9. TL-OSL and OSL-TL responses of the $CaSO_4$:Eu,Ag(a) samples.

Table 1
Medium homogeneity coefficients (C_H) and reproducibility coefficients (C_R) of produced samples.

Material	C_H (%)	C_R (%)
$CaSO_4$:Eu	8.6	7.7
$CaSO_4$:Eu,Ag(a)	5.0	1.1
$CaSO_4$:Eu,Ag(b)	7.2	6.9
$CaSO_4$:Eu,Ag(c)	14.3	22.2

intrinsic sensitivity of each dosimeter, minor variations in response were observed among them. The ratio of the TL response of each dosimeter to the mean batch response of all dosimeters results in the dosimeter homogeneity coefficient (C_H). The ratio of the TL response of the dosimeter to the average response of the 5 reading cycles results in the dosimeter reproducibility coefficient (C_R). Table 1 shows the average values of the coefficients C_H and C_R of each studied material. It is worth highlighting the great homogeneity and reproducibility of the $CaSO_4$:Eu,Ag(a) samples, which presented C_H of 5% and C_R of 1.1%.

To evaluate the linearity of the samples, only 10 dosimeters of each material with C_H less than 5% were used, except for $CaSO_4$:Eu,Ag(c) pellets, whose C_H limit was 10%, in order to have enough samples for the measurements to be performed. All samples were irradiated at doses from 85 mGy to 3.4 Gy. A linear adjustment was performed to verify the linearity range of the response. The adjustments presented almost linear correlation coefficients of 0.994 for $CaSO_4$:Eu, 0.999 for $CaSO_4$:Eu,Ag (a), 0.996 for $CaSO_4$:Eu,Ag(b) and 0.982 for $CaSO_4$:Eu,Ag(v) samples. In Fig. 10, which presents dose-response curves in a log-log plotted graph, it can be observed that the TL response of the composites showed a linear behaviour in the studied dose range. Only the $CaSO_4$:Eu,Ag(c) composites showed a non-linear TL response behaviour for doses higher than 1 Gy.

3.5. Lower detection limit and fading

The lower detection limit or lowest detectable dose (LDD) of the materials produced was calculated by the Equation $\boldsymbol{LDD} = (\overline{\boldsymbol{B}} + 3\boldsymbol{\sigma}_{\overline{\boldsymbol{B}}})\boldsymbol{f}_c$ (Oberhofer and Scharmann, 1981). In this calculation, $\overline{\boldsymbol{B}}$ is the average of the readings of 10 non-irradiated dosimeters, usually known as "background"; $\boldsymbol{\sigma}_{\overline{\boldsymbol{B}}}$ is the standard deviation of the measures of non-irradiated dosimeters and $\boldsymbol{f}_c$ is a calibration factor which represents the inverse of the slope of the dose-response curve and is expressed by Gy/arb.units. Table 2 presents the minimum detectable doses obtained

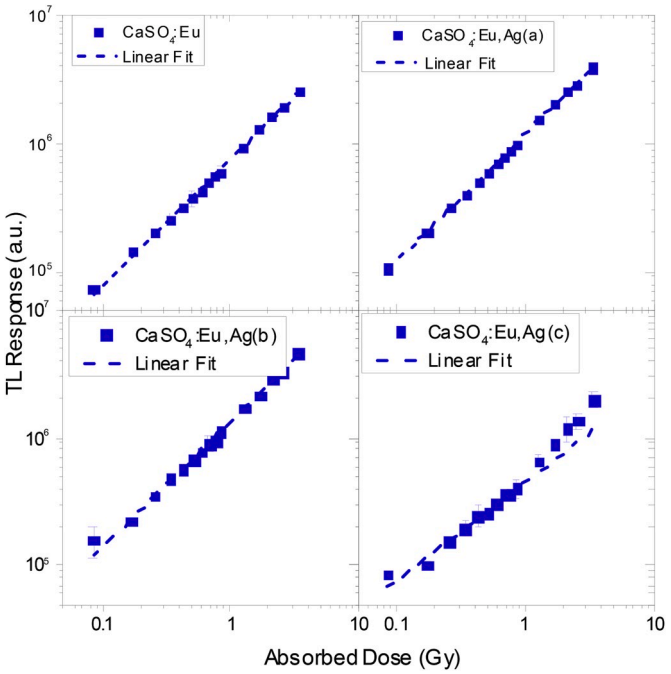

Fig. 10. TL response (area under each whole glow curve) of the $CaSO_4$:Eu, $CaSO_4$:Eu,Ag(a), $CaSO_4$:Eu,Ag(b) and $CaSO_4$:Eu,Ag(c), samples as a function of absorbed dose ($^{90}Sr/^{90}Y$).

Table 2
Minimum detectable dose of the materials produced.

Sample	Minimum detectable dose (mGy)
$CaSO_4$:Eu	8 ± 1
$CaSO_4$:Eu,Ag(a)	4 ± 1
$CaSO_4$:Eu,Ag(b)	4 ± 1
$CaSO_4$:Eu,Ag(c)	22 ± 1

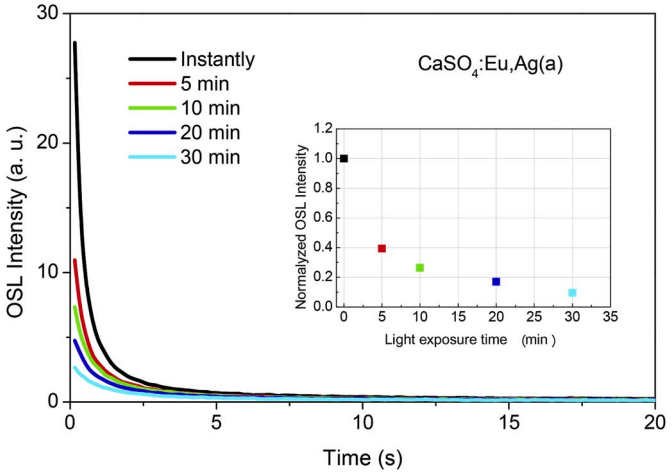

Fig. 11. Optical fading of the $CaSO_4$:Eu,Ag(a) sample irradiated with 1 Gy ($^{90}Sr/^{90}Y$).

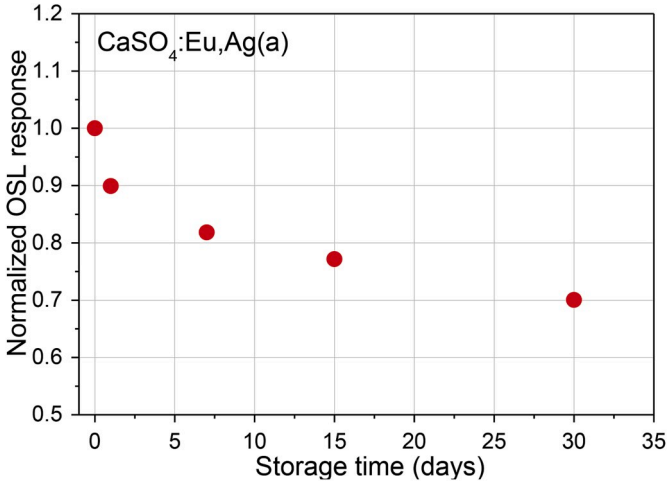

Fig. 12. Normalized OSL response of $CaSO_4$:Eu,Ag(a) samples after different storage times.

for samples irradiated with $^{90}Sr/^{90}Y$. As expected, due to their high sensitivity, $CaSO_4$:Eu,Ag(a) and $CaSO_4$:Eu,Ag(b) were the materials with the lowest detection limits (4 mGy). It is worth mentioning that the LDD depends not only on the detector, but also on the reader and on the used reading parameters (Datz et al., 2011). So, the LDDs of the samples could be considered high since the Riso reader is not a commercial device intended for low dose measurements.

OSL dosimeters are extremely sensitive to light and their optical fading is an important parameter both in the evaluation of the fade correction coefficients and in the evaluation of the optical treatment time. Fig. 11 shows OSL curves that demonstrate the optical fading of $CaSO_4$:Eu,Ag(a) samples over 30 min of exposure to ambient light. The total area under the OSL signal of the samples is reduced to 40% of the initial signal in just 5 min of exposure and over 30 min it is less than 10% of the initial signal. This evidences the high sensitivity to ambient light of this samples and indicates that there must be a rigor in the storage of this material when used as a dosimeter. The OSL fading of $CaSO_4$:Eu,Ag (a) samples under dark conditions (and room temperature) was also evaluated for a period of 30 days. Fig. 12 shows the percentual decay of the OSL signal (area under OSL curve) of the samples after storage time. The OSL signal of $CaSO_4$:Eu,Ag(a) samples decayed by 10% after one day, 18% after 7 days, 23% after 15 days, and 30% after 30 days. These results are slightly better than the 38% TL signal decay reported by Junot et al. (2014) for similar samples.

4. Conclusions

X-ray diffraction analyses showed that the production route used in the crystal growth was viable, allowing the synthesis of samples of doped $CaSO_4$ with single phase corresponding to the crystal structure of anhydride. Optical characterization confirmed the presence of Eu^{3+} and Eu^{2+} ions in the crystal matrix. The presence of silver drastically reduces the emissions related to the Eu^{3+} ion, and increases the emissions related to the Eu^{2+} ion. No emission related to Ag ions could be observed in all samples, leading to the conclusion that the silver co-doping enhances the concentration of Eu^{2+} ions in the $CaSO_4$ lattice. The $CaSO_4$:Eu,Ag(a) and $CaSO_4$:Eu,Ag(b) samples showed TL emission glow curves with two peaks centred around 170 °C and 205 °C. The $CaSO_4$:Eu,Ag(c) samples showed a peak centred around 170 °C and a low intense peak at 275 °C, possibly result of impurities due to the synthesis process. All samples presented properties useful for dosimetric purposes, such as linearity, reproducibility and lowest detectable doses in the order of mGy. Lower LDDs are important, since they enable the use of detectors in environmental and personal dosimetry, in which the measured doses are generally low. The $CaSO_4$:Eu,Ag(a) samples showed the best potential for application in OSL dosimetry, due to its higher sensitivity, approximately 40% of the Al_2O_3:C (Rexon) commercial dosimeter, considering initial OSL intensity. The radiation sources and the dose range used in the irradiations are quite common in therapeutic procedures, so that the produced dosimeters could be used in this type of monitoring, after an adequate dosimetric characterization. However, for personal dosimetry, compared to commercial TL/OSL dosimeters, it is still necessary to achieve ways to minimize the material fading. On the other hand, the produced dosimeters may also come to be used in industrial procedures in which fading is not a crucial characteristic.

Acknowledgements

The authors thank the Brazilian agencies CNEN, CNPq (Grants 155848/2018-6 and 301335/2016-8) and CAPES for their partial financial support.

References

Azorin, J., 2014. Preparation methods of thermoluminescent materials for dosimetric applications: an overview. Appl. Radiat. Isot. 83, 187–191.
Datz, H., Horowitzc, Y.S., Osterd, L., Margaliot, M., 2011. Critical dose threshold for TL dose response non-linearity: dependence on the method of analysis: it's not only the data. Radiat. Meas. 46, 1444–1447.
Guckan, V., Altunal, V., Nur, N., Depci, T., Ozdemir, A., Kurt, K., Yu, Y., Yegingil, I., Yegingil, Z., 2017. Studying $CaSO_4$:Eu as an OSL phosphor. Nucl. Instrum. Methods Phys. Res. B. 407, 145–154.
Ingle, N.B., Omanwar, S.K., Muthal, P.L., Dhopte, S.M., Kondawaret, V.K., 2008. Synthesis of $CaSO_4$:Dy, $CaSO_4$:Eu^{3+} and $CaSO_4$:Eu^{2+} phosphors. Radiat. Meas. 43, 1191–1197.
Junot, D.O., Couto dos Santos, M.A., Souza, D.N., Vasconcelos, D.F., Caldas, L.V.E., Chagas, M.A.P., 2011. Silver addition in $CaSO_4$:Eu, TL and TSEE properties. Radiat. Meas. 46, 1500–1502.
Junot, D.O., Couto dos Santos, M.A., Antonio, P.L., Caldas, L.V.E., Souza, D.N., 2014. Feasibility study of $CaSO_4$:Eu, $CaSO_4$:Eu,Ag and $CaSO_4$:Eu,Ag(NP) as thermoluminescent dosimeters. Radiat. Meas. 71, 99–103.
Kher, R.S., Pandey, R.K., Dhoble, S.J., Khokhar, M.S.K., 2011. Impulsive excitation of mecanoluminescence in gamma irradiated $CaSO_4$:Eu phosphors. Radiat. Eff. Defect Solid 116, 63–66.

Kudryavtseva, I., Klopov, M., Lushchik, A., Lushchik, C., Maaroos, A., Pishtshev, A., 2014. Electronic excitations and self-trapping of electrons and holes in $CaSO_4$. Phys. Scripta 89, 044013.
Kulkarni, M.S., Patilb, R.R., Patleb, A., Rawata, N.S., Ratnaa, P., Bhattc, B.C., Moharil, S. V., 2014. Optically stimulated luminescence from $CaSO_4$:Eu - preliminary results. Radiat. Meas. 71, 95–99.
Lakshmanan, A.R., 1999. Photoluminescence and thermostimulated luminescence processes in rare-earth-doped $CaSO_4$ phosphors. Prog. Mater. Sci. 44, 1–187.
Oberhofer, M., Scharmann, A., 1981. Applied Thermoluminescence Dosimetry. CRC Press, Ispra.
Risö, 2015. Guide to "The RisØ TL/OSL Reader". DTU Nutech, Denmark.
Yamashita, T., Nada, N., Onishi, H., Kitamura, S., 1971. Calcium sulphate phosphor activated by thulium or dysprosium for thermoluminescence dosimetry. Health Phys. 21, 295–300.
Yashaswini, Pandurangappa, C., Dhananjaya, N., Murugendrappa, M.V., 2017. Photoluminescence, Raman and conductivity studies of $CaSO_4$ nanoparticles. Int. J. Nanotechnol. 14, 845–858.